

Learning and Generalizing Variable Impedance Manipulation Skills from Human Demonstrations*

Yan Zhang, Fei Zhao, Zhiwei Liao

Abstract—By learning Variable Impedance Control policy, robot assistants can intelligently adapt their manipulation compliance to ensure both safe interaction and proper task completion when operating in human-robot interaction environments. In this paper, we propose a DMP-based framework that learns and generalizes variable impedance manipulation skills from human demonstrations. This framework improves robots' adaptability to environment changes (i.e. the weight and shape changes of grasping object at the robot end-effector) and inherits the efficiency of demonstration-variance-based stiffness estimation methods. Besides, with our stiffness estimation method, we generate not only translational stiffness profiles, but also rotational stiffness profiles that are ignored or incomplete in most learning Variable Impedance Control papers. Real-world experiments on a 7 DoF redundant robot manipulator have been conducted to validate the effectiveness of our framework.

Index Terms—Learning from Demonstrations, Variable Impedance Control, Dynamic Movement Primitives

I. INTRODUCTION

Intelligent robot assistants are increasingly expected to solve complex tasks in industrial environments and at home. Different from traditional industrial robots that complete a specific task in simple structured environments repeatedly, intelligent robot assistants may be required to perform different tasks in varying unstructured scenarios. Although Learning from Demonstration (LfD) provides ordinary users with practical interfaces to teach robots manipulation skills [1][2], an imitation learning framework with generalization ability is still needed to further reduce human intervention and to improve robots adaptation ability to environment changes. Besides, as robot assistants usually operate in human-populated environments, the manipulation compliance should also be carefully scheduled to ensure safe interaction while robots completing the target task.

Dynamic Movement Primitives (DMP) model, firstly introduced in [3] and further improved in [4],[5], becomes popular in the LfD community because of its powerful generalization ability. In general, DMP modulates each dimension of the demonstrated movement trajectory as a second-order damped spring system. By approximating the non-linear force terms and adjusting the attractor points, DMP can then generalize the demonstrated trajectory to similar situations while keeping

its overall shape. With this property, DMP has been used in various robot manipulation scenarios, such as grasping objects at different positions [4], playing drums at different heights [4], and tennis swings [6]. In these papers, by elbowing robots with generalizable manipulation skills from once kinesthetic teaching, DMP greatly reduces human intervention during robot skill acquisition. However, the manipulation compliance is still ignored in most DMP-based skill learning framework.

Impedance Control (IC) [7] is commonly introduced in robot controller design for achieving compliant motions, in which the controller can be viewed as a virtual spring-damp system between the robot end-effector and the environment. By adapting the impedance parameters based on task requirements and environment dynamics, Variable Impedance Control (VIC) can vary the manipulation compliance to ensure safe interaction and proper task completion [8]. In [9], the author proposed a Reinforcement Learning (RL) framework titled Policy Improvement with Path Integrals (PI²) where DMP was firstly integrated with impedance parameters optimization. This RL framework parameterizes the movement trajectory and impedance parameters with DMP models and then optimizes the parameters with the policy search optimization method. Different from PI² where impedance parameters are learned indirectly, the authors in [10] managed to explicitly estimate human arm stiffness profiles based on the electromyographic (EMG) signals when human performing tasks. In [11], we combined this EMG-based human arm stiffness estimation method with optimal control theory and proposed an autonomous impedance regulation framework in a class of manipulation tasks. While previously presented stiffness estimation methods show their potential in variable impedance manipulation skill acquisition, the complexity of estimating a set of parameters and the requirement of multiple EMG sensors make them inefficient and impractical for robot users.

In contrast, estimating impedance parameters from human demonstrations can be a more efficient way. In [12], the authors proposed a human-robot collaborative assembly framework where stiffness matrix is estimated by Weighted Least-Square (WLS) algorithms, with a small number of demonstrations and sensed force information. In [13], the authors considered trajectory as a virtual spring-damper system, and estimated stiffness profiles based on demonstrated kinesthetic trajectory and the associated sensed Cartesian force information. In [14], the authors also modeled trajectory with a virtual spring-damper system, but they estimated the gain parameters of this spring-damper system from demonstrated position trajectory to formulate a compliant controller. In their model, the

Yan Zhang, Fei Zhao and Zhiwei Liao are with The State Key Laboratory for Manufacturing System Engineering and Shaanxi Key Laboratory of Intelligent Robotics, School of Mechanical Engineering, Xi'an Jiaotong University, Xi'an Shaanxi, 710049, China.

This work was supported by the National Natural Science Foundation of China [Grant No. 52175029] and the Department of Science and Technology of Shaanxi Province [Grant No. 2019ZDLGY14-07]

e-mail: ztzhao@xjtu.edu.cn

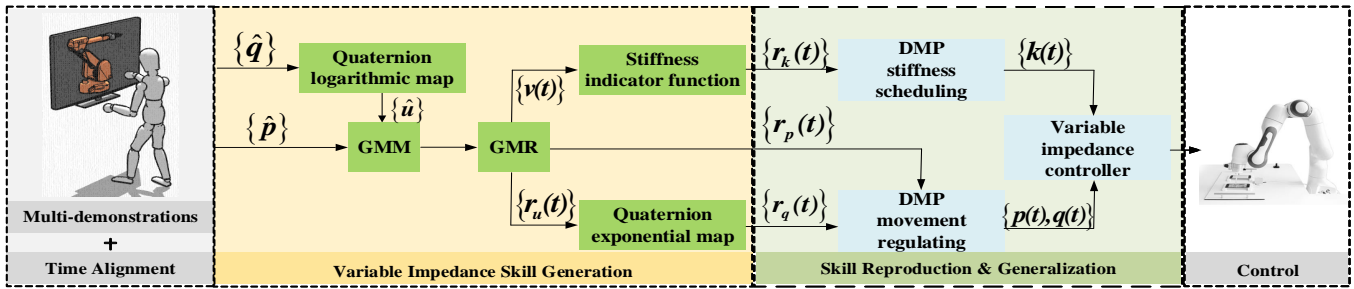


Fig. 1: The overview of our proposed learning framework.

demonstrated position trajectory distribution is generated with the Gaussian Mixture Model-Gaussian Mixture Regression (GMM-GMR) algorithm [15],[16], and the stiffness profiles are shaped so that the robot changes to a high stiffness in directions of low variance. In [17], this stiffness adaptation method is further applied to online decrease stiffness profiles when humans perturbing the robot end-effector around its equilibrium point. However, most previously presented methods mainly focus on estimating translational stiffness, rotational stiffness is ignored.

In this paper, we modified the stiffness estimation method in [14] by integrating quaternion logarithmic mapping function. This modification allows us to transform quaternions into decoupled 3D tangent vectors and then to estimate rotational stiffness profiles based on the variances of tangent vectors. Besides, we noticed most works in robot variable impedance manipulation skill learning focus on variable impedance skill reproducing and trajectory generalization, while the stiffness profiles are seldom generalized. In this paper, we argue that generalizing stiffness profiles like trajectory can further improve robots' adaptability to environment changes. To this end, we extend the classical DMP motion trajectory scheduling equations with stiffness generalization parts. The resulted learning framework is similar to the one presented in [18] where joint stiffness profiles are estimated with EMG signals and then generalized in joint space. The main differences between us are that: 1) in our work, we estimate stiffness profiles from human demonstrations, which is more practical and efficient than EMG-based methods. 2) More importantly, we learn and generalize variable impedance manipulation skills in Cartesian space. This is a more natural way to regulate trajectory and stiffness profiles, as the goals for skill generalization and the task constraints are normally presented in Cartesian space.

This paper is organized as follows. In Section 2, we introduce the methodology with the overview of our learning framework shown in Fig.1; In Section 3, we show the real-world validation experiments and analyze the results; In Section 4 and Section 5, we discuss and conclude this paper.

II. METHODOLOGY

As shown in Fig.1, our learning framework mainly consists of four parts: *Trajectory Collecting*, *Variable Impedance Skill Generation*, *Skill Reproduction and Generalization*, and *Real-world Robot Control*.

Trajectory Collecting: a human demonstrator demonstrates to the robot how to accomplish one specific task several times. Then, the demonstrated trajectories are collected and aligned into the same time scale.

Variable Impedance Skill Generation: we transform the aligned quaternions $\{\hat{q}\}$ into tangent vectors $\{\hat{u}\}$ through the Quaternion Logarithmic Mapping Function. Then, we use GMM-GMR to encode both $\{\hat{u}\}$ and $\{\hat{p}\}$ to obtain the trajectory distribution. The mean of $\{\hat{u}\}$ is then transformed back to quaternions with the Quaternion Exponential Mapping Function. Meanwhile, the variances of demonstrations are mapped to the reference stiffness profiles $\{r_k(t)\}$ with the Stiffness Indicator Function.

Skill Reproduction and Generalization: the extended DMP framework mainly consists of two parts: DMP movement regulation block and DMP stiffness scheduling block. DMP movement regulation block generalizes the generated reference pose trajectory $\{r_p(t), r_q(t)\}$ to new scenarios and DMP stiffness scheduling block regulates the reference stiffness profiles $\{r_k(t)\}$ to adapt to environment changes. Then, the torque commands are calculated based on VIC equation with $\{r_p(t), r_q(t)\}$ and $\{r_k(t)\}$.

Real-world Control: The calculated torque commands are then sent to real-world robots through Robot Operation System (ROS).

A. Pre-processing

At first, N trajectories consist of positions and orientations of the end-effector are collected through kinesthetic teaching. Each demonstration $O_i(t) = \{p_i(t_j), q_i(t_j)\}$, $i = 1, 2, \dots, N$ is a $M_i \times 7$ matrix, where M_i indicates the total number of datapoints of the i^{th} demonstrated trajectory, $p_i(t_j) = \{p_{i,x}(t_j), p_{i,y}(t_j), p_{i,z}(t_j)\}$ and $q_i(t_j) = \{q_{i,w}(t_j), q_{i,x}(t_j), q_{i,y}(t_j), q_{i,z}(t_j)\}$ represent the position and unit quaternion of i^{th} trajectory at t_j timestep, respectively. Next, we align the collected trajectories into the same time scale $[0, T]$, for a given $T > 0$. This time alignment process is done as follows: assume t_0 and t_1 be the initial and final time of a given trajectory $O_i(t)$. The aligned trajectory is then represented as:

$$\hat{O}_i(t) = O_i\left(\frac{T(t-t_0)}{t_1-t_0}\right), i = 1, 2, \dots, N \quad (1)$$

with $\hat{O}_i(t) = \{\hat{p}_i(t_j), \hat{q}_i(t_j)\}$.

B. Variable Impedance Skill Generation

1) *Quaternion Logarithmic and Exponential Mapping Functions*: Unlike positional part, there is no minimal and singularity-free representation for orientational part. The stiffness estimation method in [14] is effective to estimate translational stiffness profiles from position trajectories. However, it might not be feasible to encode orientation trajectories and estimate rotational stiffness information directly. Inspired by Quaternion-based DMP framework in [19][20], where Quaternion Logarithmic Mapping Function is applied to calculate the 3D decoupled distance vector between two quaternions, in this paper, we also utilize this mapping function to transform quaternions into decoupled 3D vectors. The generated 3D vectors can be considered as the distance vectors between the transformed quaternion and the original quaternion $\mathbf{1}=(1, 0, 0, 0)$. Besides, Quaternion Exponential Mapping Function is also presented here to transform the distance vectors back into quaternions for orientation trajectory encoding and generalization with the extended DMP framework later.

Given an unit quaternion, the Quaternion Logarithmic Map Function ($S^3 \rightarrow R^3$) is written as:

$$\hat{\mathbf{u}} = \log(\hat{\mathbf{q}}) = \begin{cases} \arccos(\hat{q}_w) \frac{(\hat{q}_x, \hat{q}_y, \hat{q}_z)}{\|(\hat{q}_x, \hat{q}_y, \hat{q}_z)\|}, & (\hat{q}_x, \hat{q}_y, \hat{q}_z) \neq \vec{0} \\ (0, 0, 0), & \text{otherwise} \end{cases} \quad (2)$$

Correspondingly, the Quaternion Exponential Map Function ($R^3 \rightarrow S^3$) is defined by:

$$\hat{\mathbf{q}} = \exp(\hat{\mathbf{u}}) = \begin{cases} (\cos \|\hat{\mathbf{u}}\|, \frac{\sin \|\hat{\mathbf{u}}\|}{\|\hat{\mathbf{u}}\|} \bullet \hat{\mathbf{u}}), & \hat{\mathbf{u}} \neq (0, 0, 0) \\ \mathbf{1}=(1, 0, 0, 0), & \text{otherwise} \end{cases} \quad (3)$$

where $\hat{\mathbf{u}} = (\hat{u}_x, \hat{u}_y, \hat{u}_z) \in T_1 S^3 \equiv R^3$ represents a tangent vector in the tangent space $T_1 S^3$.

In Eq. (3), the exponential map transforms a tangent vector $\hat{\mathbf{u}}$ into a unit quaternion $\hat{\mathbf{q}}$, a point in S^3 at distance $\|\hat{\mathbf{u}}\|$ from $\mathbf{1}$ along the geodesic curve beginning from $\mathbf{1}$ in the direction of $\hat{\mathbf{u}}$. Additionally, when we limit $\|\hat{\mathbf{u}}\| < \pi$ and $\hat{\mathbf{q}} \neq (-1, 0, 0, 0)$, these two mapping is continuously differentiable and inverse to each other.

2) *Stiffness Indicator Function*: The stiffness indicator function maps the variances of demonstrated trajectories to stiffness profiles. The basic idea is that: in the region where demonstrated-trajectory has a low variance, the robot should keep at a high stiffness level to track the reference trajectory precisely. While for the high variance parts, the robot can keep at a relatively low stiffness level to ensure manipulation compliance. To generate relatively lower stiffness profiles, we apply the left part of a quadratic function with a positive quadratic coefficient as the stiffness indicator function:

$$k_l(t) = a_l(d_l(t) - d_l^{\max})^2 + k_l^{\min} \quad (4)$$

$$a_l = \frac{k_l^{\max} - k_l^{\min}}{(d_l^{\min} - d_l^{\max})^2} > 0$$

where k_l^{\min}, k_l^{\max} are the minimal and maximal translational or rotational stiffness values in direction $l \in \{x, y, z\}$, given

based on the robot hardware limitations and real-world task constraints. Besides, d_l^{\min}, d_l^{\max} indicate the minimum and maximum of the standard deviation of the demonstrated trajectories in direction l .

C. Skill Reproduction and Generalization

1) *Extended DMP Model*: DMP model considers a trajectory as a second-order damped spring system with a non-linear force term $f(\bullet)$, like Eq.(5). Given a demonstrated trajectory, by solving the regression problem of the non-linear force term, DMP can imitate this trajectory and generalize it to new similar scenarios by adjusting the goals. However, when transferring human skills to robots, most classical DMP only encodes pose trajectories, which may lose part of the compliance of demonstrated skills. To learn and generalize compliant variable impedance manipulation skills, we extend the original DMP model by integrating the stiffness scheduling equations in Eq.(6). Meanwhile, Quaternion-based DMP, Eq. (7) is united in our extended model to encode the reference orientation trajectory.

$$\tau \mathbf{y} = \alpha_p(\beta_p(\mathbf{p}_g - \mathbf{p}) - \mathbf{y}) + \mathbf{f}_p(x) \quad (5)$$

$$\tau \mathbf{z} = \alpha_k(\beta_k(\mathbf{k}_g - \mathbf{k}) - \mathbf{z}) + \mathbf{f}_k(x) \quad (6)$$

$$\tau \dot{\boldsymbol{\eta}} = \alpha_q(\beta_q 2 \log(\mathbf{q}_g * \bar{\mathbf{q}}) - \boldsymbol{\eta}) + \mathbf{f}_q(x) \quad (7)$$

$$\tau \mathbf{p} = \mathbf{y} \quad (8)$$

$$\tau \mathbf{k} = \mathbf{z} \quad (9)$$

$$\tau \dot{\mathbf{q}} = \frac{1}{2} \boldsymbol{\eta} * \mathbf{q} \quad (10)$$

where $\mathbf{p}, \mathbf{p}_g \in R^3$ indicate current position of the robot's end-effector in Cartesian space and the final goal position; $\mathbf{k}, \mathbf{k}_g \in R^6$ represent the main diagonal elements of stiffness matrix and their target values, respectively; $\mathbf{q}, \mathbf{q}_g \in S^3$ are robot's current orientation and the final goal orientation; $\alpha_p, \alpha_k, \alpha_q, \beta_p, \beta_k, \beta_q$ are constant parameters; τ indicates the time scaling factor that is used to adjust the duration of the task; \mathbf{y}, \mathbf{z} represent position velocity, the derivative of stiffness, and the tangent vector calculated by the quaternion logarithmic map in Eq. (2); $\dot{\mathbf{q}}$ is the quaternion derivative that satisfies Eq.(10), where $\boldsymbol{\eta}$ is the angular velocity; Besides, $\bar{\mathbf{q}}$ denotes the quaternion conjugation, with the definition: $\bar{\mathbf{q}} = (q_w, -q_x, -q_y, -q_z)$. Finally, the symbol $*$ indicates the quaternion product.

The whole extended DMPs model is synchronized by the canonical system:

$$\tau \dot{x} = -\alpha_x x \quad (11)$$

where x is the phase variable to avoid explicit time dependency; α_x is a positive constant and $x(0)$ is set as 1.

The non-linear forcing terms $\mathbf{f}_p(x), \mathbf{f}_q(x), \mathbf{f}_k(x)$ are functions of x and can be regressed with Locally Weighted Regression (LWR) algorithm:

$$\mathbf{f}(x) = \frac{\sum_{s=1}^S \boldsymbol{\theta}_s \psi_s(x_j)}{\sum_{s=1}^S \psi_s(x_j)} \quad (12)$$

where $\mathbf{f}(x)$ represents $\mathbf{f}_p(x), \mathbf{f}_q(x), \mathbf{f}_k(x)$ in general. S is the number of radial basis functions used.

Given demonstrated trajectories, S-column parameter matrix θ can be obtained by solving the following equations:

$$\mathbf{f}_p(x_j) = \mathbf{G}_p^{-1}(\tau^2 \mathbf{p}_j + \tau \alpha_p (\mathbf{p}_j - \alpha_p \beta_p (\mathbf{p}_g - \mathbf{p}_j))) \quad (13)$$

$$\mathbf{f}_k(x_j) = \mathbf{G}_k^{-1}(\tau^2 \mathbf{k}_j + \tau \alpha_k (\mathbf{k}_j - \alpha_k \beta_k (\mathbf{k}_g - \mathbf{k}_j))) \quad (14)$$

$$\mathbf{f}_q(x_j) = \mathbf{G}_q^{-1}(\tau \boldsymbol{\eta}_j - \alpha_q (\beta_q 2 \log(\mathbf{q}_g * \bar{\mathbf{q}}_j) - \boldsymbol{\eta}_j)) \quad (15)$$

$$\psi_s(x) = \exp(-h_s(x - c_s)^2) \quad (16)$$

where $\mathbf{G}_p = \text{diag}(\mathbf{p}_g - \mathbf{p}_0) \in R^{3 \times 3}$, $\mathbf{G}_k = \text{diag}(\mathbf{k}_g - \mathbf{k}_0) \in R^{6 \times 6}$, $\mathbf{G}_q = \text{diag}(2 \log \mathbf{q}_g - \mathbf{q}_0) \in R^{3 \times 3}$ are spatial scaling factors. h_s, c_s are the width and center of Gaussian distribution $\psi_s(x)$.

2) *Variable Impedance Control*: With the scheduled pose trajectory $\{\mathbf{p}, \mathbf{q}\}$ and stiffness profiles \mathbf{k} , we can calculate the command torques based on the variable impedance control equation:

$$\boldsymbol{\Gamma} = \mathbf{J}^T (\mathbf{K} \mathbf{e} + \mathbf{D} \dot{\mathbf{e}}) + \boldsymbol{\Gamma}_{ff} \quad (17)$$

where the stiffness matrix $\mathbf{K} = \text{diag}(\mathbf{k}) \in R^{6 \times 6}$ and damping matrix $\mathbf{D} = \sqrt{2\mathbf{K}}$; \mathbf{J} is the Jacobian matrix, $\boldsymbol{\Gamma}$ represents the joint torque and $\boldsymbol{\Gamma}_{ff}$ is the joint torque contributed by feed-forward term. $\mathbf{e}, \dot{\mathbf{e}}$ denote the reference pose trajectory tracking error and tracking velocity.

III. EXPERIMENTAL EVALUATION

In this section, the 7DoF Franka Emika Robot(Panda) is used in our experimental study. For all the experiments, Panda is controlled under libfranka scheme with 1kHz control frequency. A toy task, serving drinks is illustrated to show that our framework 1) learns a reasonable variable impedance manipulation skill from human demonstrations; 2) enables the robot to generalize the reference stiffness profiles to adapt to the changes of the robot end-effector.

As discussed in [20], pouring the content of a bottle into a cup can be done with kinematic control model. However, in human-populated environments, a person may incautiously push the robot while it reaching for the cup. A stiff controller will respond with high forces, which may hurt the user and cause the liquid to spill. It would thus be desirable to control the way that the robot responds to translational and rotational perturbations.

In the real world, human tends to gradually increase the translational and rotational stiffness while reaching the cup and keep at high stiffness while pouring drinks. Besides, humans can also easily adapt to the shape and weight changes of the grasping bottle. In this experiment, we show that our framework learns reasonable variable impedance manipulation skills and also enables Panda to adapt to the weight and shape changes of the bottle like humans, by endowing it with variable impedance manipulation skill generalization ability.

The experiment set up is shown in Fig.2. Panda is expected to 1) pour water from a 0.25 kg plastic bottle into the middle cup on the table by reproducing the demonstrated pose

trajectory and stiffness profiles; 2) pour water into the other two cups by generalizing the reference pose trajectory; 3) pour wine from a 0.9 kg glass bottle into the cups by generalizing the reference trajectory and stiffness profiles simultaneously.



Fig. 2: Experiment setup

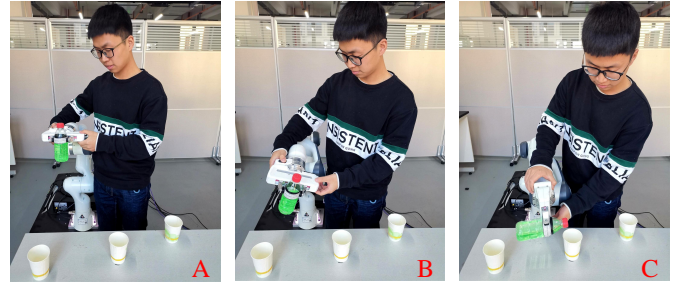


Fig. 3: Kinesthetic teaching. The robot user demonstrates Panda how to pour water into the middle cup.

A. Learning Variable Impedance Manipulation Skill

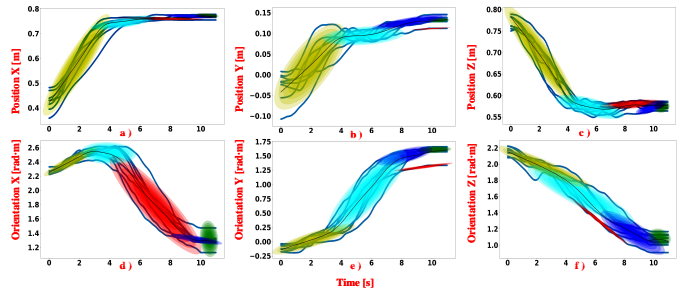


Fig. 4: GMM-GMR encodes the positional and orientational datapoints. The demonstrated trajectories, the estimated mean functions, and the trained Gaussian kernels are marked with blue lines, black lines, and colorful ellipses, respectively.

We first show Panda how to pour water into the middle cup on the table 8 times in slightly different situations, with kinesthetic teaching (Fig.3). Then, the collected pose trajectories were aligned into the same time scale $T = 11$ seconds. Next, we transformed the unit quaternions into tangent vectors with the Quaternion Logarithmic Mapping Function, Eq.(2), and encoded both positional and orientational datapoints with

GMM-GMR, with $H=6$ Gaussian components, shown in Fig.4. Finally, the mean tangent vectors in Fig.4 (d-f) were converted back into unit quaternions through the Quaternion Exponential Mapping Function, Eq.(3).

The reference stiffness profiles is estimated with our Stiffness Indicator Function, Eq.(4), based on the variances of the demonstrated trajectories. For pouring water experiment, the minimal and maximal translational stiffness values allowed are set as $k^{\min} = 200N/m$ and $k^{\max} = 550N/m$, and the values for the rotational stiffness are $k^{\min} = 10N/(rad \bullet m)$, $k^{\max} = 20N/(rad \bullet m)$. The estimated stiffness profiles are presented together with the standard deviations of the collected trajectories in Fig.5.

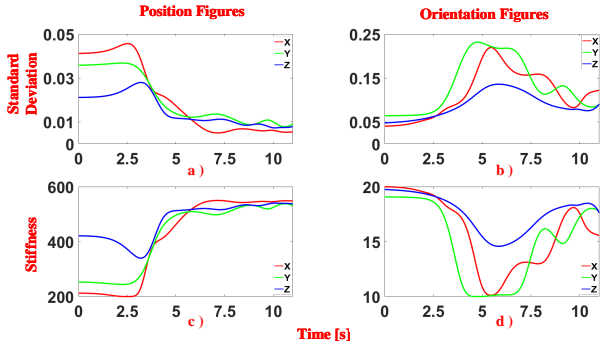


Fig. 5: a-b) represent the standard deviation of the collected motion trajectories; c-d) show the estimated stiffness profiles

Overall, the estimated translational stiffness profiles increase when the robot reaching for the cup and keep high when pouring water. Before beginning the experiment, we expect the rotational stiffness profiles show the same tendency to the translational part. Nevertheless, they actually start from high values, decrease gradually at around 3s and keep increasing to high values from around 7s until the end. This tendency is actually more reasonable than what we expected. At the beginning phase of pouring water, we unconsciously perform high rotational stiffness to avoid our hand rotate to prevent the water from spilling out. Therefore, our framework can indeed generate reasonable stiffness profiles from human demonstrations.

To illustrate we successfully transferred the stiffness features to Panda in the real world, we recorded the mean tracking errors of pouring water into the middle cup with 1)the estimated stiffness profiles, 2)the minimal stiffness value allowed, 3) the maximal stiffness value allowed. The result is shown in Fig.6

We firstly set rotational stiffness at $20N/(rad \bullet m)$, then used $200N/m$, $550N/m$ and the reference translational stiffness profiles to accomplish the pouring water experiment for 3 times for each translational stiffness mode. The mean positional errors were shown in the upper 3 graphs in Fig.6. It is noticeable that our variable impedance controller behaves like a $200 N/m$ constant stiffness controller from 0s to around 4s, as the yellow lines are close to the blue lines during this period. After 4s, the yellow lines almost coincide with the red lines which represent the tracking errors of the $550 N/m$

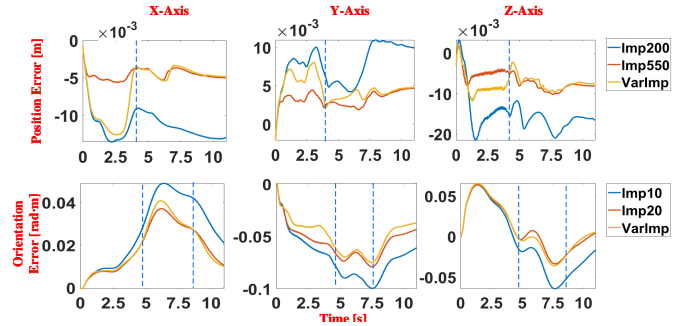


Fig. 6: Comparison of mean tracking pose errors in different stiffness modes

constant stiffness controller. This exactly reflects the tendency of the translational stiffness in Fig.5c). As for the rotational part, we set the translational stiffness at $550 N/m$, and tested the mean tracking errors of $10N/(rad \bullet m)$, $20N/(rad \bullet m)$, and the reference orientational stiffness profiles. The results are shown in the lower 3 graphs in Fig.6. The results also inflict the overall tendency of the orientational stiffness in Fig.5d). Therefore, with our extended-DMP model, Panda learns reasonable variable impedance manipulation pouring water skill.

B. Variable Impedance Skill Generalization

In this section, we generalize the learned variable impedance manipulation skill to new scenarios and show our extended-DMP model further improves Panda's adaptability to the shape and weight changes of the grasping bottle. First, we used the reference stiffness profiles and generalized the pose trajectory to show our framework inherits the motion generalization ability of DMP model. As shown in Fig.7, with the generalized pose trajectory, Panda can successfully pour water into the three cups on the table with a similar trajectory shape.

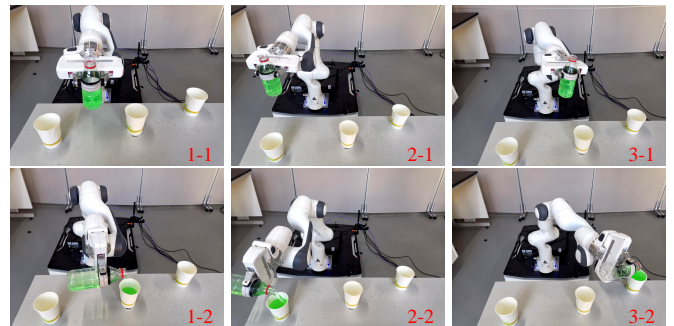


Fig. 7: Shortcuts of real-world pouring water experiment

Then, we replaced the light plastic bottle with a heavier glass wine bottle. As the wine bottle is longer than the plastic one, this will require different goal poses for pouring wine into the same cups. The generalized pose trajectories for pouring wine are shown in Fig.8.

When we executed the new pose trajectories with the reference stiffness profiles for pouring water, Panda failed to

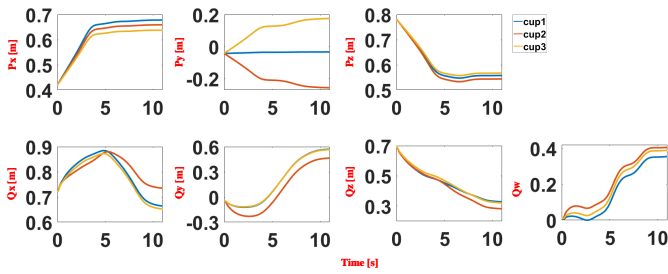


Fig. 8: Generalized pose trajectories for pouring wine task

pour wine into the first cup and the third cup, and managed to pour wine into the second cup only once, shown in Fig.9 a). The main reasons for this failure are that: 1) the glass bottle is heavier than the plastic one. The reference translational stiffness profiles should be increased to compensate for the mass change of the robot end-effector, particularly the stiffness in Axis Z; 2) A longer bottle will enlarge the positional distance errors between the cup and the bottleneck when there are orientational errors. Besides, a heavier bottle also introduced larger external torques at the end-effector. Therefore, the values of rotational stiffness should be increased correctly to compensate for the external torques and to reduce the orientational tracking errors. Meanwhile, no matter it is pouring water or pouring wine, the overall stiffness shape should be kept, as the task constraints did not change for the pouring tasks.

Therefore, we generalized both the stiffness profiles to new goal values and keep its overall tendency with Eq.(6). We re-run the pouring wine tests for 3 times. Panda successfully adapted the changes and managed to pour wine into the cups, just like what we have shown in Fig.7

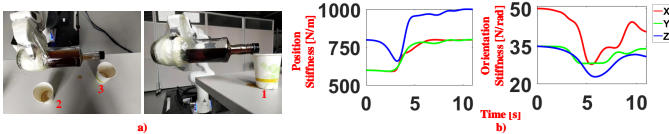


Fig. 9: a) Performance of the reference pouring water stiffness profiles in pouring wine task. Panda did not reach the range for pouring wine and even crushed the cup. b) Generalized stiffness profiles that accomplished the pouring wine task

IV. DISCUSSION

It should be emphasized that our stiffness estimation method estimates both translational and rotational stiffness profiles, while most previously presented methods can not achieve this goal. Another advantage of our method is its efficiency and effectiveness while estimating stiffness profiles. In this paper, with only 8 collected trajectories, we could generate reasonable stiffness profiles to reproduce the demonstrated skill and to further generalize it to new scenarios.

Besides, in this article, we mainly focus on learning and generalizing stiffness profiles from human demonstrations. However, the estimated stiffness profiles may not be optimal for the target task. Improving the stiffness profiles with optimization methods, like PI^2 [9], can be useful to further

improve the performance of the learned variable impedance manipulation skill in solving the target task.

V. CONCLUSION

In this work, we proposed an efficient DMP-based imitation learning framework for learning and generating variable impedance manipulation skills from human demonstrations in Cartesian space. This framework not only estimates both translational and rotational stiffness profiles from demonstrated trajectories, but also improves robots' adaptability to environment changes (i.e. the weight and shape changes of the robot's end-effector) by generalizing generated stiffness profiles. The experimental study validates the effectiveness of our proposed framework. Besides, we believe it can be used on robots with different configurations, as our framework learns and generalizes skills in Cartesian space.

For future work, we will test our proposed approach in more complex human-robot interaction tasks. It is also an interesting direction to further optimize the generated reference trajectory and stiffness profiles through reinforcement learning algorithms.

REFERENCES

- [1] Aude Billard, Sylvain Calinon, Ruediger Dillmann, and Stefan Schaal. Survey: Robot programming by demonstration. Technical report, Springer, 2008.
- [2] Sylvain Calinon. *Robot programming by demonstration*. EPFL Press, 2009.
- [3] Auke Jan Ijspeert, Jun Nakanishi, and Stefan Schaal. Trajectory formation for imitation with nonlinear dynamical systems. In *Proceedings 2001 IEEE/RSJ International Conference on Intelligent Robots and Systems. Expanding the Societal Role of Robotics in the the Next Millennium (Cat. No. 01CH37180)*, volume 2, pages 752–757. IEEE, 2001.
- [4] Heiko Hoffmann, Peter Pastor, Dae-Hyung Park, and Stefan Schaal. Biologically-inspired dynamical systems for movement generation: Automatic real-time goal adaptation and obstacle avoidance. In *2009 IEEE International Conference on Robotics and Automation*, pages 2587–2592. IEEE, 2009.
- [5] Auke Jan Ijspeert, Jun Nakanishi, Heiko Hoffmann, Peter Pastor, and Stefan Schaal. Dynamical movement primitives: learning attractor models for motor behaviors. *Neural computation*, 25(2):328–373, 2013.
- [6] Auke Jan Ijspeert, Jun Nakanishi, and Stefan Schaal. Learning attractor landscapes for learning motor primitives. Technical report, 2002.
- [7] Neville Hogan. Impedance control: An approach to manipulation: Part i—theory. 1985.
- [8] Aleš Ude, Andrej Gams, Tamim Asfour, and Jun Morimoto. Task-specific generalization of discrete and periodic dynamic movement primitives. *IEEE Transactions on Robotics*, 26(5):800–815, 2010.
- [9] Jonas Buchli, Freek Stulp, Evangelos Theodorou, and Stefan Schaal. Learning variable impedance control. *The International Journal of Robotics Research*, 30(7):820–833, 2011.
- [10] Arash Ajoudani, Nikos Tsagarakis, and Antonio Bicchi. Tele-impedance: Teleoperation with impedance regulation using a body-machine interface. *The International Journal of Robotics Research*, 31(13):1642–1656, 2012.
- [11] Yuqiang Wu, Fei Zhao, Tao Tao, and Arash Ajoudani. A framework for autonomous impedance regulation of robots based on imitation learning and optimal control. *IEEE Robotics and Automation Letters*, 6(1):127–134, 2020.
- [12] Leonel Rozo, Sylvain Calinon, Darwin Caldwell, Pablo Jiménez, and Carme Torras. Learning collaborative impedance-based robot behaviors. In *Proceedings of the AAAI conference on artificial intelligence*, volume 27, 2013.
- [13] Fares J Abu-Dakka, Leonel Rozo, and Darwin G Caldwell. Force-based variable impedance learning for robotic manipulation. *Robotics and Autonomous Systems*, 109:156–167, 2018.

- [14] Sylvain Calinon, Irene Sardellitti, and Darwin G Caldwell. Learning-based control strategy for safe human-robot interaction exploiting task and robot redundancies. In *2010 IEEE/RSJ International Conference on Intelligent Robots and Systems*, pages 249–254. Citeseer, 2010.
- [15] Zoubin Ghahramani and Michael I Jordan. Supervised learning from incomplete data via an em approach. In *Advances in neural information processing systems*, pages 120–127, 1994.
- [16] Sylvain Calinon, Florent Guenter, and Aude Billard. On learning, representing, and generalizing a task in a humanoid robot. *IEEE Transactions on Systems, Man, and Cybernetics, Part B (Cybernetics)*, 37(2):286–298, 2007.
- [17] Klas Kronander and Aude Billard. Online learning of varying stiffness through physical human-robot interaction. In *2012 IEEE International Conference on Robotics and Automation*, pages 1842–1849. Ieee, 2012.
- [18] Chenguang Yang, Chao Zeng, Cheng Fang, Wei He, and Zhijun Li. A dmps-based framework for robot learning and generalization of humanlike variable impedance skills. *IEEE/ASME Transactions on Mechatronics*, 23(3):1193–1203, 2018.
- [19] Aleš Ude, Bojan Nemeč, Tadej Petrič, and Jun Morimoto. Orientation in cartesian space dynamic movement primitives. In *2014 IEEE International Conference on Robotics and Automation (ICRA)*, pages 2997–3004. IEEE, 2014.
- [20] Peter Pastor, Ludovic Righetti, Mrinal Kalakrishnan, and Stefan Schaal. Online movement adaptation based on previous sensor experiences. In *2011 IEEE/RSJ International Conference on Intelligent Robots and Systems*, pages 365–371. IEEE, 2011.